Plasmon-Enhanced Polymer-Sensitized Solar Cells

ARTICLE *in* THE JOURNAL OF PHYSICAL CHEMISTRY C · FEBRUARY 2015

Impact Factor: 4.77 · DOI: 10.1021/jp5097458

THE JOURNAL OF PHYSICAL CHEMISTRY C

Article

pubs.acs.org/JPCC

Plasmon-Enhanced Polymer-Sensitized Solar Cells

Simon Sandén,[†,‡] Kenta Akitsu,[‡] Björn Törngren,[§] Anne Ylinen,[†] Jan-Henrik Smått,[§] Takaya Kubo,[‡] Mitsunobu Matsumura,[∥] Naoki Otani,[∥] Hiroshi Segawa,[‡] and Ronald Österbacka*[,†]

[†]Physics, Department of Natural Sciences and Center for Functional Materials, Åbo Akademi University, Porthansgatan 3, 20500 Turku, Finland

[‡]Research Center for Advanced Science and Technology, The University of Tokyo, 4-6-1, Komaba, Meguro-ku, Tokyo 153-8904, Japan

[§]Laboratory of Physical Chemistry, Department of Natural Sciences and Center for Functional Materials, Åbo Akademi University, Porthansgatan 3, 20500 Turku, Finland

[∥]Electronic Materials Research Department, Nissan Chemical Industry, Ltd., 488-6, Suzumi-cho, Funabashi-shi, Chiba 274-0052, Japan

ABSTRACT: Plasmon-enhanced polymer-sensitized solar cells were manufactured by incorporating core−shell Au@SiO_2 particles into the TiO_2 photoanode. The plasmon-enhanced solar cells showed an improved performance due to an increased j_{sc} leading to a higher power conversion efficiency compared to reference devices without Au@SiO_2 particles, and a small increase in the V_{oc} was also observed. The incident photon to current efficiency (IPCE) spectra showed that an enhanced absorption in the plasmon devices was the cause of the improved performance. By electrodynamics modeling of the Au@SiO_2 particles, we conclude that a combination of scattering and near-field enhancement is the cause of the increased efficiency in these plasmon-enhanced solar cells.

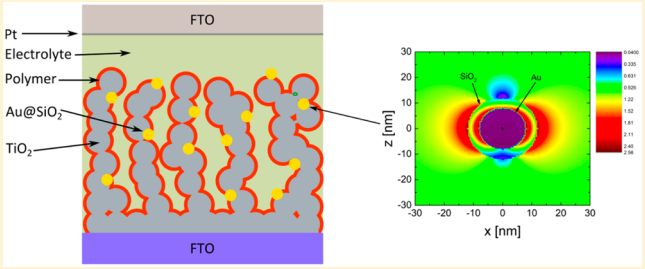

INTRODUCTION

Solar energy is the most abundant source of renewable energy at our disposal. Traditional silicon-based solar cells have been used for over half a century. Although the power generation cost of silicon-based solar cells has been decreasing, high production and installation costs resulting in long payback time are important issues to be solved for their widespread use. As a result of this, research in third-generation photovoltaics has seen a huge surge in the last decades due to its use of low-cost materials and the possibility to utilize high-throughput printing methods in the processing.

The dye-sensitized solar cell (DSSC) is a promising candidate for large-scale electricity production.[1] A DSSC consists of a mesoporous titanium dioxide (TiO_2) layer onto which a light-absorbing dye is attached. Charges are generated when photons are absorbed by the dye and inject an electron into the TiO_2 layer which is then transported to the cathode, while the hole left on the dye is transported by an electrolyte or hole transport layer. Due to the operation mechanism in DSSCs, i.e., absorption in the dye and electron (hole) transport in the TiO_2 (electrolyte), light harvesting and charge transport can be optimized separately.

The commonly used sensitizers in DSSCs giving the high performance are ruthenium complexes.[2] Ru complexes typically show low optical absorption coefficients, which require thicker mesoporous TiO_2 layers to increase the light-harvesting efficiency. Efforts to replace the Ru-containing complexes have been made due to the high cost of Ru. Organic donor−π-acceptor porphyrin dyes, which do not contain any expensive elements, have been synthesized and used in high efficiency DSSCs.[3] Replacing the dye used in DSSCs with π-conjugated polymers has also been used in DSSCs.[4,5] The advantage with polymers is that they can be synthesized using abundant materials and typically show large absorption coefficients. In addition to this, polymers can form thicker layers due to the folding of the polymer chain. The polymer thickness is limited by the short exciton diffusion length encountered in these materials, typically being in the 5−10 nm range.[6,7] This, however, is much thicker than the monolayer of dye coverage in standard DSSCs meaning that the thickness of the photoactive layer can be reduced when using polymer sensitizers.

One major issue with DSSCs is the low efficiency (<12%) compared to conventional silicon solar cells (~20%). This low efficiency is mainly due to poor mismatch between absorption in the solar cells and the solar spectrum, thus limiting the overall light absorption; this is especially true in polymer-sensitized solar cells. One recent approach to increase absorption in the red part of the spectrum has been to utilize surface plasmons to enhance absorption in solar cells[8−12]

Received: September 26, 2014
Revised: February 19, 2015
Published: February 23, 2015

DOI: 10.1021/jp5097458
J. Phys. Chem. C 2015, 119, 5570−5576

meaning that the thickness of the device and the materials cost to produce the cell can be substantially reduced.[13] This enhancement in light absorption can be attributed to the near-field or far-field effects of the nanoparticles, depending on the particle size.[14]

We have recently studied the effects of adding plasmonic gold nanoparticles to the photoanode of a DSSC.[15] Plasmonic core–shell particles were added to the mesoporous TiO_2 layer of a DSSC, which resulted in an increased efficiency compared with conventional devices. In the present study, we have utilized the same concept by adding plasmonic core–shell nanoparticles to a mesoporous TiO_2 layer sensitized with polythiophene derivatives. We have measured the photovoltaic properties of the devices and related the enhancing effects to a combination of near-field and far-field (scattering) enhancement arising from the plasmonic particles using modeling of the electromagnetic fields of the core–shell particles.

EXPERIMENTAL SECTION

Polymer Synthesis and Hydrolysis. The copolymer poly[(methylthiophene-3-yl-carboxylate)-*ran*-(thiophene)] (PT-MC) (see Figure 1) was synthesized by dehalogenation

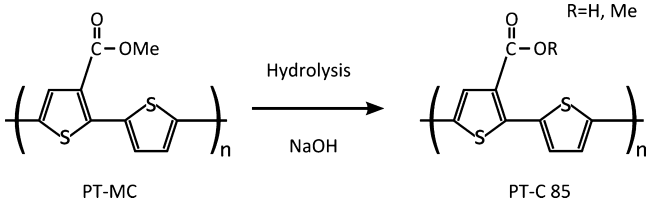

Figure 1. Partial hydrolysis of the PT-MC polymer using NaOH to obtain the PT-C polymer with a hydrolysis ratio ([COOH]/([COOH] + [COOMe])) of 85%.

polymerization of a 2:1 mixture of diethyl 2,5-dibromothiophene-3-ylcarboxylate and 2,5-dibromothiophene in the presence of a $Ni(cod)_2$ catalyst. A PT-MC polymer with a mean molecular weight of 2300 g/mol was obtained using this synthesis protocol. Hydrolysis of the PT-MC polymer was performed using NaOH to obtain a polymer with a hydrolysis ratio, defined as [COOH]/([COOH] + [COOMe]), of 85%, hereafter referred to as PT-C 85 (see Figure 1). A detailed description of the polymer synthesis can be found in the work of Kubo et al.[16]

Core–Shell Particle Fabrication. Core–shell Au@SiO_2 particles were synthesized using wet chemical methods. The gold nanoparticle cores were synthesized according to the method by Turkevich et al.[17] An aqueous solution (500 mL) of 0.5 mM gold(III) chloride hydrate was brought to boil. Sodium citrate (2.5 mL, 1 mM) was added, and the solution was left to boil for 30 min. The solution turned from light yellow to ruby red in a few minutes, indicating the formation of citrate-capped Au nanoparticles. To improve the nanoparticle stability in nonaqueous solutions, the capping agent was exchanged. A fresh, aqueous solution of polyvinylpyrrolidone (PVP) (12.8 mg/mL) was prepared, and 3.2 mL of the solution was added to the Au nanoparticles under vigorous stirring. The solution was left to react for 24 h under stirring, and thereafter centrifuged and washed with water.

A protective and insulating SiO_2 shell was coated on the PVP-capped Au nanoparticles using a method modified from the one presented by Obare et al.[18] A fresh 3-mercaptopropyl trimethoxysilane solution was prepared (10 μL in 1 mL of ethanol), and 200 μL was added to 25 mL of the aqueous Au nanoparticle solution and stirred for 20 min. An aqueous 0.54 wt % sodium silicate solution (pH 10–11) was prepared, and 800 μL was added to the Au nanoparticles, stirred for 20 min, and allowed to sit for 12 h. The nanoparticle solution was thereafter centrifuged at 10 000 rpm and washed with water and ethanol three times.

Transmission electron microscopy (TEM) images of the core–shell nanoparticles were taken with a JEOL JEM-2200FS operating at a 200 kV acceleration voltage. The optical properties of the synthesized nanoparticles were characterized by absorption spectroscopy using a Shimadzu UV-2501PC. The absorption of Au@SiO_2 particles in PT-C 85 solutions was characterized using a Shimadzu UV-3600 spectrophotometer, and the photoluminescence was characterized using a Shimadzu RF-503 spectrofluorophotometer.

TiO_2 + Au@SiO_2 Paste Fabrication. A viscous TiO_2 paste used for screen-printing the photoanodes was prepared following a modified method reported by Ito et al.[19] Briefly, 0.1 g of P25 TiO_2 (Degussa) nanoparticles was mixed with 0.4 g of α-terpineol. To this mixture, 0.033 g of ethyl cellulose dissolved in 0.1 g of ethanol was added and mixed for 12 h. For the plasmonic samples, Au@SiO_2 nanoparticles dispersed in ethanol were added corresponding to 1% Au, by weight, to the resulting paste. The mixture was vigorously shaken, and the excess solvent was evaporated to achieve proper viscosity for screen-printing.

Solar Cell Fabrication and Characterization. Solar cell devices were made by screen-printing the TiO_2 paste, with or without addition of Au@SiO_2 nanoparticles, onto a FTO glass to obtain an area of 0.16 cm^2. The TiO_2 films were sintered at 500 °C for 30 min and subsequently immersed into a 0.1 mg/mL solution of PT-C 85 in dimethyl sulfoxide (DMSO) for 20 h to form a thin homogeneous polymer layer on the mesoporous TiO_2 structure. A complete polymer-sensitized solar cell (PSSC) was assembled by sandwiching a Himilian spacer between the photoanodes and a platinum-coated FTO glass and injecting I^-/I_3^- liquid electrolyte (0.5 M tetra-*n*-butyl ammonium iodide, 25 mM I_2 in acetonitrile) between the electrodes. A schematic of the completed solar cell is shown in Figure 2.

Current–voltage (j–V) characteristics of the assembled PSSCs were measured under AM 1.5G simulated solar light using a solar simulator (Bunko-keiki, CEP-2000) to obtain the solar cell parameters: power conversion efficiency (η), short-

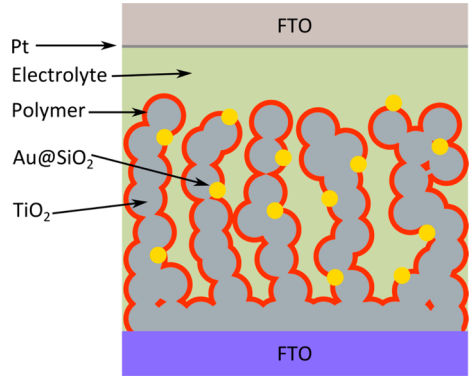

Figure 2. Schematic of the device structure of the polymer-sensitized solar cell.

DOI: 10.1021/jp5097458
J. Phys. Chem. C 2015, 119, 5570–5576

circuit current density (j_{sc}), open-circuit voltage (V_{oc}), and fill factor (FF). The incident photon to current efficiency (IPCE) spectra were measured using a monochromator equipped with a 150 W Xe lamp (Bunko-keiki, CEP-2000).

Model. The benefits of adding nanoparticles to DSSCs can be analyzed by modeling the electromagnetic field around core−shell particles. The light-scattering properties of spherical nanoparticles are described using Mie theory for spherical particles.[20] In Mie theory the incident electromagnetic radiation is modeled as a plane wave with a certain wavelength. The particle is spherically symmetric with respect to the chosen origin and can have an arbitrary number of layers. The particle is described by its wavelength-dependent complex refractive index and its size.

The electromagnetic fields inside and outside the particle can be expressed as a superposition of spherical harmonic functions and Bessel functions. By demanding continuity of electric and magnetic field components one can solve for the expansion coefficients and obtain an exact expression for the electromagnetic fields. The expansion coefficients are functions of wavelength, particle size, and the refractive index of the particle. With knowledge of the expansion coefficients it is possible to evaluate different properties of the modeled material as presented below.

Using a far-field approximation the scattering (Q_{sca}) and absorption (Q_{abs}) coefficients can be calculated. The scattering coefficient describes how much of the light incident on the particle is scattered by the particle. Similarly the absorption coefficient describes how much of the incident light is absorbed by the particle. The extinction coefficient, $Q_{ext} = Q_{sca} + Q_{abs}$, can be compared to absorption measurements for synthesized particles.

The near-field coefficient, Q_{NF}, is an indicator of how large the electromagnetic fields are close to the surface of a particle. The near-field coefficient has a definition similar to that of the scattering coefficient, but it is evaluated at the surface of the particle. A high Q_{NF} can be assumed to correlate with increased photocurrents, as larger electromagnetic fields close to the particle lead to the dye/polymer absorbing more light.[21]

In the calculations, a program by Bohren and Huffman[22] was modified according to suggestions by Yang[23] and used to obtain Q_{sca} and Q_{abs}. The near-field coefficient was calculated using the expression of Messinger.[24] The refractive indexes for the materials used in calculations were obtained from Johnson and Christy.[25]

RESULTS AND DISCUSSION

Core−shell Au@SiO_2 nanoparticles have been fabricated using the methods described above. This synthesis procedure resulted in core−shell nanoparticles with a 16 nm diameter gold core and a 4 nm thick SiO_2 shell as shown in Figure 3a. The importance of a complete SiO_2 shell has been shown to be vital to ensure stability of the gold core toward the corrosive I^-/I_3^- electrolyte used in dye-sensitized solar cells.[15] The absorption spectrum of the synthesized Au@SiO_2 particles dispersed in ethanol is shown in Figure 3b, where the characteristic plasmon resonance peak has a maximum at 530 nm.

To clarify if the absorption and/or photoluminescence of the PT-C 85 polymer can be enhanced by the addition of Au@SiO_2 particles, solutions of mixtures of these two materials were prepared at increasing concentration of Au@SiO_2. The polymer and nanoparticles were dispersed in dimethyl sulfoxide (DMSO) at a polymer concentration of 0.01 mg/mL. Both

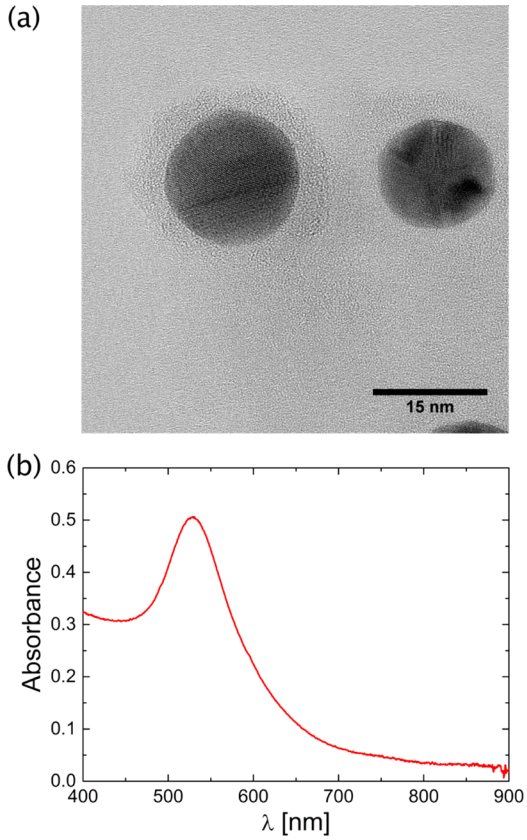

Figure 3. (a) TEM image of the core−shell Au@SiO_2 particles showing a 16 nm diameter gold core coated with a 4 nm thick SiO_2 shell and (b) absorption spectrum of the core−shell Au@SiO_2 particles in ethanol.

materials were dispersible in this solvent without any chemical modifications to either the polymer or the nanoparticles. The absorption spectra of mixtures with 0, 5, 10, and 20 wt % Au@SiO_2 in relation to PT-C 85 are shown in Figure 4. An increase in the absorption for all Au@SiO_2 concentrations can be seen as expected. The absorption enhancement given by the difference

$$\Delta\text{Abs} = \text{Absorbance}\ (n\ \text{wt}\ \%) - \text{Absorbance}\ (0\ \text{wt}\ \%) \quad (1)$$

where n = 5, 10, and 20 wt % is shown in Figure 4b, from which it can be seen that a large enhancement is located on the red side of the plasmon resonance peak. This indicates that the absorption near the polymer absorption onset can be enhanced by the addition of Au@SiO_2 particles. Increasing the light harvesting close to the polymer's optical gap is desirable as the absorption is typically low in this wavelength range, thus having a low contribution to the current generation in solar cell devices.[4,16] The photoluminescence (PL) of the same solutions was also measured. These PL spectra for the mixtures excited at 510 nm (direct excitation of the plasmon) are shown in Figure 5a. Here it can be seen that also the photoluminescence is increasing by adding Au@SiO_2 particles to the polymer solutions. The enhancement of the photoluminescence by addition of the core−shell particles has been evaluated by the ratio

$$\text{PL}_{\text{enh}} = \frac{\int_{525}^{800} \text{PL}\ (n\ \text{wt}\ \%)}{\int_{525}^{800} \text{PL}\ (0\ \text{wt}\ \%)} \quad (2)$$

DOI: 10.1021/jp5097458
J. Phys. Chem. C 2015, 119, 5570−5576

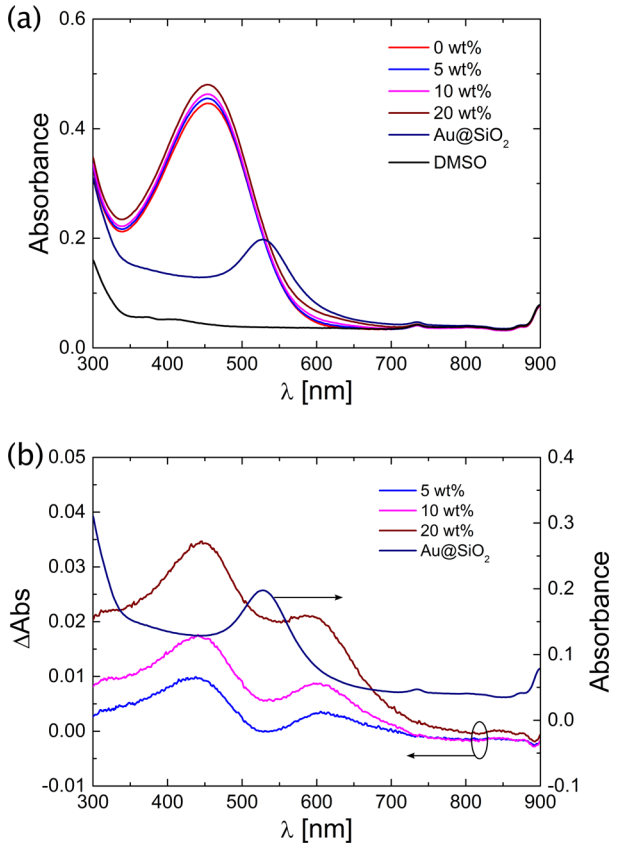

Figure 4. (a) Absorption spectra of mixtures of PT-C 85 and Au@SiO_2 particles in DMSO at 0 (red line), 5 (blue line), 10 (pink line), and 20 wt % (brown line) Au@SiO_2:PT-C85 and the absorption spectra of npAu@SiO_2 particles (dark blue line) (the contributions to the spectra from the solvent DMSO are shown by including the absorption of the solvent (black line) showing a peak at 740 and 900 nm) and (b) the absorption enhancement caused by addition of an increasing amount of npAu@SiO_2 as evaluated according to eq 2.

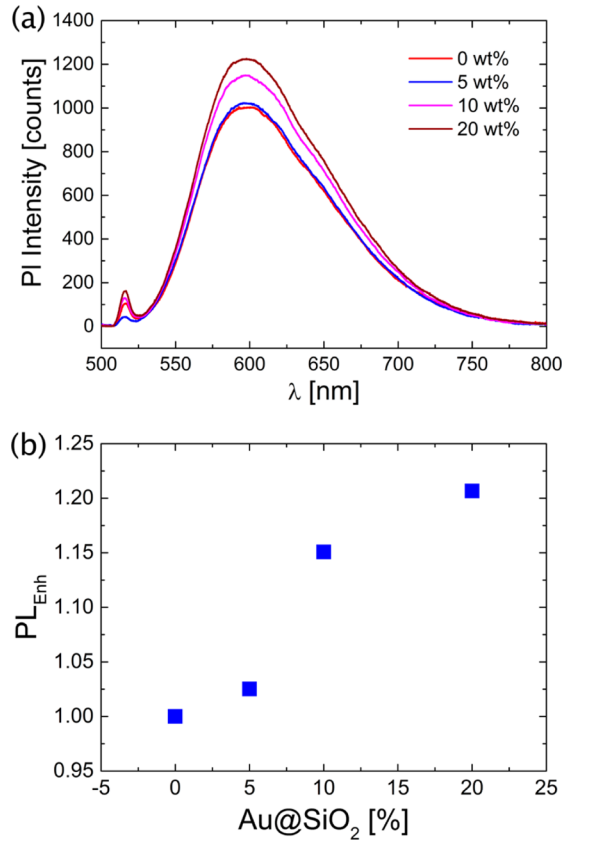

Figure 5. (a) Photoluminescence spectra of PT-C 85 and Au@SiO_2 mixtures in DMSO at different Au@SiO_2 concentrations and (b) the photoluminescence increase when adding Au@SiO_2 particles to the PT-C85 solution.

where n= 5, 10, and 20 wt %. The small peak around 510 nm caused by the scattering of light from the excitation at 510 nm has been disregarded to avoid errors in the estimation of the PL intensity. The PL enhancement as a function of Au@SiO_2 amount is presented in Figure 5b, showing that the addition of Au@SiO_2 particles results in an increase in the PL intensity. This increased intensity indicates that a larger amount of excitons is formed by the addition of Au@SiO_2 which is expected to lead to an increase in charges generated in solar cell devices. The absorption and photoluminescence measurements indicate that photoexcitations in the PT-C 85 polymer will be enhanced due to the addition of plasmonic nanoparticles and lead to an increase in the performance of polymer-sensitized solar cells. The estimation of the distance between the polymer and the particles is difficult due to the fact that both will diffuse around in the solution. However, as the concentrations of polymer and Au@SiO_2 in the solutions are rather low (~0.01 mg/mL), some attractive interaction forces between the polymer and the silica shell might explain the relatively high enhancement seen in both the absorption and the PL. It should be highlighted that the pure Au@SiO_2 dispersion showed no discernible PL when excited at 510 nm.

Plasmon-enhanced polymer-sensitized solar cells (*plasmon*), incorporating 1 wt % Au@SiO_2 in the TiO_2 photoanode and reference devices (*reference*) without Au@SiO_2 particles were fabricated as described previously. The $j-V$ curves of *plasmon* and *reference* devices measured under simulated sunlight are shown in Figure 6 at different TiO_2 photoanode thicknesses.

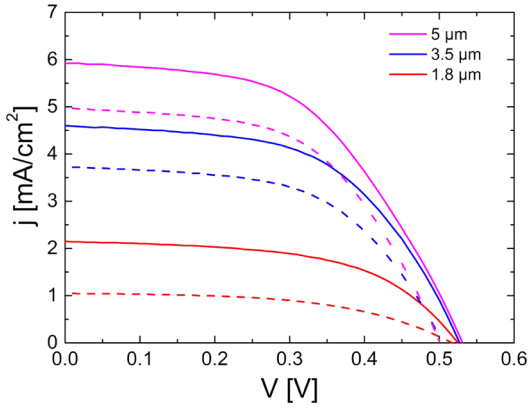

Figure 6. Representative $j-V$ curves for *plasmon* (solid line) and TiO_2 *reference* (dashed) devices.

Here it can be seen that all *plasmon* devices show a higher current compared to the *reference* devices. The solar cell parameters of the devices in Figure 6 are shown in Table 1 where the average performance and the standard deviation are given. Here it can be seen that j_{sc} has increased in all the plasmon devices with a slight variation in the FF of the solar cells. A slight increase in the V_{oc} is also seen in all *plasmon*

DOI: 10.1021/jp5097458
J. Phys. Chem. C 2015, 119, 5570−5576

Table 1. Average Solar Cell Device Parameters of *Plasmon* (Au) and *Reference* (Ref) Devices[a]

sample	V_{oc} (V)	FF	j_{sc} (mA/cm^2)	η (%)
ref 1	0.52 ± 0.01	0.54 ± 0.04	2.04 ± 1.4	0.58 ± 0.43
Au 1	0.56 ± 0.05	0.56 ± 0.01	2.7 ± 0.8	0.87 ± 0.35
ref 2	0.51 ± 0.01	0.55 ± 0.01	4.14 ± 0.6	1.2 ± 0.2
Au 2	0.54 ± 0.02	0.54 ± 0.01	4.55 ± 0.08	1.32 ± 0.01
ref 3	0.50 ± 0.01	0.54 ± 0.01	5.3 ± 0.4	1.42 ± 0.10
Au 3	0.53 ± 0.01	0.51 ± 0.01	6.0 ± 0.1	1.62 ± 0.01

[a]The numbers after the sample name correspond to the thickness of the devices: 1.8, 3.5, and 5 μm for 1, 2, and 3, respectively (N = 2).

devices. Choi et al.[26] demonstrated that the charging of Au@TiO_2 particles will lead to a Fermi-level shift and thus a V_{oc} increase. However, the use of an insulating SiO_2 shell will prevent this effect. However, we note that the Fermi level in TiO_2 is very sensitive to extrinsic effects such as charging doping and so on which can lead to a shift in the V_{oc} which in our case can be due to charging of the SiO_2 shell used in the *plasmon* devices leading to an increased V_{oc}. The addition of core−shell particles into the mesoporous TiO_2 layer has also been shown to decrease backward electron transfer, thereby increasing the V_{oc}.[27] The highest enhancement in the performance of the solar cells is seen in the device with the thinnest (1.8 μm) TiO_2 layer (50% increase in efficiency), while the enhancement decreases as the TiO_2 layer is increased to 3.5 and 5 μm (~13% increase in both cases).

The increase in power conversion efficiency is correlated with the increase in the IPCE spectra as shown in Figure 7a where a broad increase in the spectra can be seen for all plasmon-enhanced devices. The enhancement in the *plasmon* devices has been evaluated by taking the ratio

$$\Delta\mathrm{IPCE} = \frac{\mathrm{IPCE}_{\mathrm{plasmon}}(\lambda)}{\mathrm{IPCE}_{\mathrm{reference}}(\lambda)} \quad (3)$$

The IPCE enhancement for the devices having thicknesses of 3.5 and 5 μm is shown in Figure 7b (the enhancement for the 1.8 μm device is shown in the inset) from which it can be seen that the largest enhancement is observed around 560 nm. We note that the highest increase is located on the red side of the plasmon resonance peak as also observed in Figure 4b; however, we point out that the redshift in solution is much larger than when characterizing the solid TiO_2 photoanode. We speculate that these differences can be caused by the different preparation methods leading to the observed discrepancies.

To obtain insight into how the Au@SiO_2 particles affect the enhancement increase of the solar cells studied in this work, the far-field and near-field properties of these particles have been simulated using the model presented earlier. The scattering (far-field) coefficient (Q_{sca}) and near-field coefficient (Q_{NF}) for Au@SiO_2 particles with a 16 nm gold core and 4 nm SiO_2 shell as a function of wavelength are shown in Figure 8a. Here it can be seen that the maximum of the near-field coefficient is slightly red-shifted compared to the maximum of the scattering coefficient. From Figure 8a we observe that the magnitude of Q_{NF} is much higher than Q_{sca} by over 3 orders of magnitude. However, near-field effects can only affect the absorption enhancement when the absorbing dye is in close proximity to the core−shell particle. To clarify in what range near-field enhancement can be expected to take place we have modeled the intensity enhancement of a core−shell particle as shown in

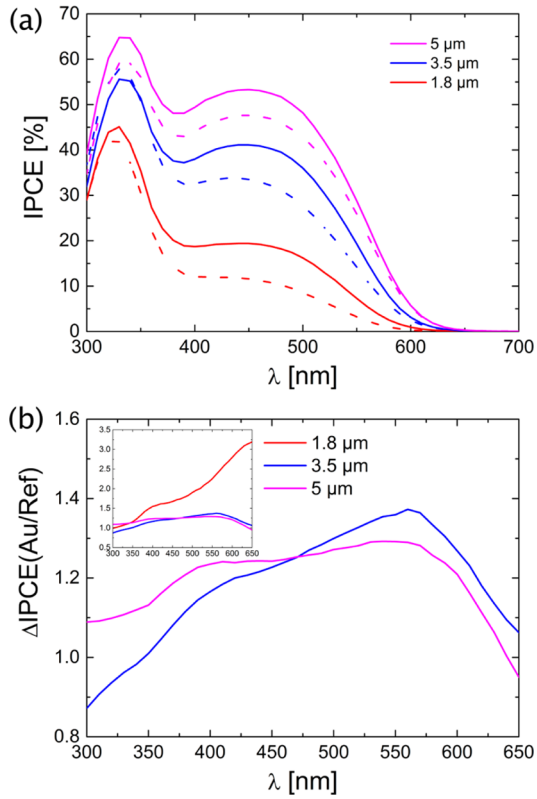

Figure 7. (a) Representative IPCE spectra for the *plasmon* (solid) and TiO_2 *reference* (dashed) devices at different thicknesses and (b) the IPCE enhancement for the 3.5 and 5 μm thick devices showing a maximum enhancement at 560 nm. The enhancement including the 1.8 μm device is shown in the inset.

Figure 8b, where light at 520 nm incident upon the particle along the z-axis excites the plasmon resonance leading to increased fields near the surface of the particle. From the figure it can be seen that a strong enhancement is obtained within a distance of 5 nm from the outside of the SiO_2 shell, visualized by the red shaded half circle area in Figure 8b. This indicates that if near-field enhancement of the absorption is to take place in the solar cell, the core−shell particles must be in close vicinity of an absorbing polymer/dye. Since the core−shell particles used in this work have been dispersed into the TiO_2 paste as shown schematically in Figure 2, and therefore are located on the surface of the mesoporous TiO_2, we can expect that the polymer adsorbed onto the TiO_2 will be in close proximity to the Au@SiO_2 for near-field enhancement to take place. We cannot completely rule out additional chemical or structural effects due to residual surfactant or synthetic byproducts from the nanoparticle synthesis. Nevertheless, due to our triple washing procedure we believe such effects will be minimal. In addition to the near-field enhancement of the absorption we note that the magnitude for scattering coefficient of the Au@SiO_2 particles increases for wavelengths shorter than 480 nm, and since an increase in the ΔIPCE was seen around 400 nm in Figure 7b we postulate that scattering is the cause of this increase. We therefore conclude that the increase in absorption in these PSSCs is due to a combination of near-field absorption enhancement and increased optical path length due to scattering.

DOI: 10.1021/jp5097458
J. Phys. Chem. C 2015, 119, 5570−5576

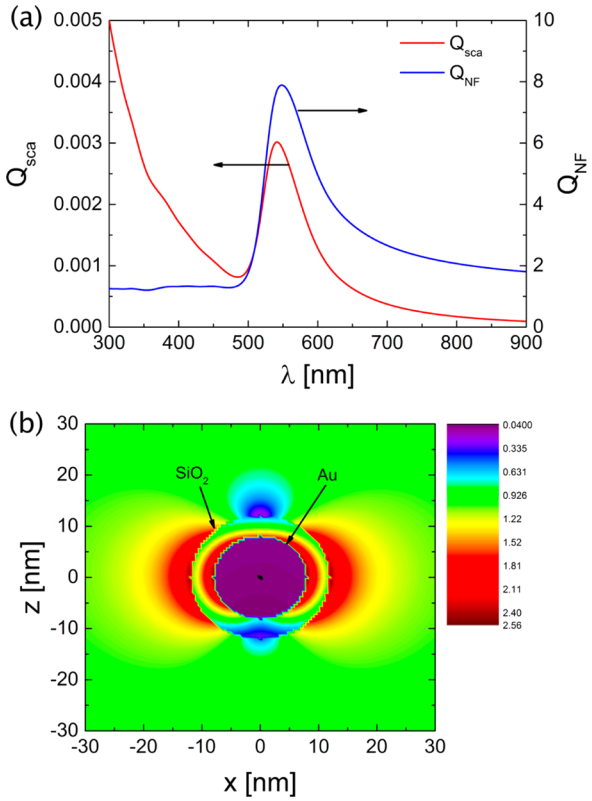

Figure 8. (a) Scattering constant Q_{sca} and the near-field constant Q_{NF} and (b) a 2-D plot of the near-field intensity enhancement for a Au@SiO_2 particle with a 16 nm gold core and 4 nm SiO_2 shell at excitation at 520 nm.

CONCLUSIONS

Core−shell Au@SiO_2 particles which show a plasmon resonance peak at 530 nm have been synthesized. By integrating these particles into polymer-sensitized solar cells, we obtained plasmon-enhanced solar cells which showed an improved performance due to the increased j_{sc}. The amplified current appeared due to the larger amount of absorbed photons as seen in the increased IPCE spectra for all plasmon-enhanced devices. The modeling of the near-field and far-field behavior in Au@SiO_2 particles shows that the enhancement is due to a combination of near-field and far-field (scattering) effects, which leads to an increased absorption of photons.

AUTHOR INFORMATION

Corresponding Author

*E-mail: rosterba@abo.fi.

Notes

The authors declare no competing financial interest.

ACKNOWLEDGMENTS

Financial support from the Academy of Finland project No. 37093 (POHSC) is acknowledged by S.S and B.T. R.Ö. acknowledges a personal grant from the Swedish Cultural Foundation in Finland. S.S. acknowledges the Fortum Foundation, the Magnus Ehrnroth Foundation, the Finnish Foundation for Technology Promotion, the Swedish Academy of Engineering Sciences in Finland, and the Scandinavia-Japan Sasakawa Foundation. The Japan Society for the Promotion of Science (JSPS) through its Funding Program for World-Leading Innovative R&D on Science and Technology (FIRST Program) is acknowledged.

REFERENCES

(1) O'Regan, B.; Grätzel, M. A Low-Cost, High-Efficiency Solar Cell Based on Dye-Sensitized Colloidal TiO_2 Films. *Nature* **1991**, *353*, 737−740.

(2) Nazeeruddin, M. K.; Angelis, F. D.; Fantacci, S.; Selloni, A.; Viscardi, G.; Liska, P.; Ito, S.; Takeru, B.; Grätzel, M. Combined Experimental and DFT-TDDFT Computational Study of Photoelectrochemical Cell Ruthenium Sensitizers. *J. Am. Chem. Soc.* **2005**, *127*, 16835−16847.

(3) Yella, A.; Lee, H.-W.; Tsao, H. N.; Yi, C.; Chandiran, A. K.; Nazeeruddin, M. K.; Diau, E. W.-G.; Yeh, C.-Y.; Zakeeruddin, S. M.; Grätzel, M. Porphyrin-Sensitized Solar Cells with Cobalt (II/III)−Based Redox Electrolyte Exceed 12% Efficiency. *Science* **2011**, *334*, 629−634.

(4) Akitsu, K.; Kubo, T.; Uchida, S.; Segawa, H.; Otani, N.; Tomura, M.; Tamura, T.; Matsumura, M. Polymer-Sensitized Solar Cells Using Polythiophene Derivatives with Directly Attached Carboxylic Acid Groups. *Jpn. J. Appl. Phys.* **2012**, *51*, 10NE04-1-6.

(5) Fang, Z.; Eshbaugh, A. A.; Schanze, K. S. Low-Bandgap Donor−Acceptor Conjugated Polymer Sensitizers for Dye-Sensitized Solar Cells. *J. Am. Chem. Soc.* **2001**, *133*, 3063−3069.

(6) Theander, M.; Yartsev, A.; Zigmantas, D.; Sundström, V.; Mammo, W.; Andersson, M. R.; Inganäs, O. Photoluminescence Quenching at a Polythiophene/C60 Heterojunction. *Phys. Rev. B* **2000**, *61*, 12957−12963.

(7) Goh, C.; Scully, S. R.; McGehee, M. D. Effects of Molecular Interface Modification in Hybrid Organic-Inorganic Photovoltaic Cells. *J. Appl. Phys.* **2007**, *101*, 114503-1−114503-12.

(8) Sheehan, S. W.; Noh, H.; Brudvig, G. W.; Cao, H.; Schmuttenmaer, C. A. Plasmonic Enhancement of Dye-Sensitized Solar Cells Using Core−Shell−Shell Nanostructures. *J. Phys. Chem. C* **2013**, *117*, 927−934.

(9) Xu, Q.; Liu, F.; Meng, W.; Huang, Y. Plasmonic Core-Shell Metal-Organic Nanoparticles Enhanced Dye-Sensitized Solar Cells. *Opt. Express* **2012**, *20*, A898−A907.

(10) Puche, D.; Torchio, P.; Escoubas, L.; Monestier, F.; Simon, J.-J.; Flory, F.; Mathian, G. Improving Light Absorption in Organic Solar Cells by Plasmonic Contribution. *Sol. Energy Mater. Sol. Cells* **2009**, *93*, 1377−1382.

(11) Wu, J.-L.; Chen, F.-C.; Hsiao, Y.-S.; Chien, F.-C.; Chen, P.; Kuo, C.-H.; Huang, M. H.; Hsu, C.-H. Surface Plasmonic Effects of Metallic Nanoparticles on the Performance of Polymer Bulk Heterojunction Solar Cells. *ACS Nano* **2011**, *5*, 959−967.

(12) Yang, J.; You, J.; Chen, C.-C.; Hsu, W.-C.; Tan, H.-R.; Zhang, X. W.; Hong, Z.; Yang, Y. Plasmonic Polymer Tandem Solar Cell. *ACS Nano* **2011**, *5*, 6210−6217.

(13) Nakayama, K.; Tanabe, K.; Atwater, H. A. Plasmonic Nanoparticle Enhanced Light Absorption in GaAs Solar Cells. *Appl. Phys. Lett.* **2008**, *93*, 121904−1−121904−3.

(14) Myroshnychenko, V.; Rodriguez-Fernandez, J.; Pastoriza-Santos, I.; Funston, A. M.; Novo, C.; Mulvaney, P.; Liz-Marzan, L.-M.; Javier Garcia de Abajo, F. Modelling the Optical Response of Gold Nanoparticles. *Chem. Soc. Rev.* **2008**, *37*, 1792−1805.

(15) Törngren, B.; Akitsu, K.; Ylinen, A.; Sandén, S.; Jiang, H.; Ruokolainen, J.; Komatsu, M.; Hamamura, T.; Nakazaki, J.; Kubo.; et al. Investigation of Plasmonic Gold−Silica Core−Shell Nanoparticle Stability in Dye-Sensitized Solar Cell Applications. *J. Colloid Interface Sci.* **2014**, *427*, 54−61.

(16) Kubo, T.; Akitsu, K.; Uchida, S.; Segawa, H.; Otani, N.; Tomura, M.; Tamura, T.; Matsumura, M. Polymer-sensitized Solar Cells with Novel Soluble Polythiophene Derivatives. *J. Photopolym. Sci. Technol.* **2010**, *33*, 283−286.

(17) Turkevich, J.; Stevenson, P. C.; Hillier, J. The Formation of Colloidal Gold. *J. Phys. Chem.* **1953**, *57*, 670−673.

DOI: 10.1021/jp5097458
J. Phys. Chem. C 2015, 119, 5570−5576

(18) Obare, S.; Jana, N. R.; Murphy, C. J. Preparation of Polystyrene- and Silica-Coated Gold Nanorods and Their Use as Templates for the Synthesis of Hollow Nanotubes. *Nano Lett.* **2001**, *1*, 601−603.
(19) Ito, S.; Chen, P.; Compte, P.; Nazeeruddin, M. K.; Liska, P.; Péchy, P.; Grätzel, M. Fabrication of Screen-Printing Pastes from TiO_2 Powders for Dye-Sensitized Solar Cells. *Prog. Photovoltaics: Res. Appl.* **2007**, *15*, 603−612.
(20) Mie, G. Beiträge zur Optik Trüber Medien, Speziell Kolloidaler Metallösungen. *Ann. Phys.* **1908**, *330*, 377−445.
(21) Brown, M. D.; Suteewong, T.; Kumar, R. S. S.; D'Innocenzo, V.; Petrozza, A.; Lee, M. M.; Weisner, U.; Snaith, H. J. Plasmonic Dye-Sensitized Solar Cells Using Core−Shell Metal−Insulator Nanoparticles. *Nano Lett.* **2011**, *11*, 438−445.
(22) Bohren, C. F.; Huffman, D. R. *Absorption and Scattering of Light by Small Particles*; John Wiley & Sons, Inc.: New York, Chichester, Brisbane, Toronto, Sydney, 1983.
(23) Yang, W. Improved Recursive Algorithm for Light Scattering by a Multilayered sphere. *Appl. Opt.* **2003**, *42*, 1710−1720.
(24) Messinger, B. J.; von Raben, K. U.; Chang, R. K.; Barber, P. W. Local Fields at the Surface of Noble-Metal Microspheres. *Phys. Rev. B* **1981**, *24*, 649−657.
(25) Johnson, P. B.; Christy, R. W. Optical Constants of the Noble Metals. *Phys. Rev. B* **1972**, *6*, 4370−4379.
(26) Choi, H.; Chen, W. T.; Kamat, P. V. Know Thy Nano Neighbor. Plasmonic Versus Electron Charging Effects of Metal Nanoparticles in Dye-Sensitized Solar Cells. *ACS Nano* **2006**, *6*, 4418−4427.
(27) Ding, B.; Lee, B. J.; Yang, M.; Jung, H. S.; Lee, J. K. Surface-Plasmon Assisted Energy Conversion in Dye-Sensitized Solar Cells. *Adv. Energy Mater.* **2011**, *1*, 415−421.

DOI: 10.1021/jp5097458
J. Phys. Chem. C 2015, 119, 5570−5576